

Suppression of Dielectronic Recombination Due to Finite Density Effects

D. Nikolić¹, T. W. Gorczyca, K. T. Korista

Western Michigan University, Kalamazoo, MI, USA

G. J. Ferland

University of Kentucky, Lexington, KY, USA

and

N. R. Badnell

University of Strathclyde, Glasgow, UK

Received _____; accepted _____

¹Department of Mechanical Engineering, University of Alberta, Edmonton AB, Canada

ABSTRACT

We have developed a general model for determining density-dependent effective dielectronic recombination (DR) rate coefficients in order to explore finite-density effects on the ionization balance of plasmas. Our model consists of multiplying by a suppression factor those highly-accurate total zero-density DR rate coefficients which have been produced from state-of-the-art theoretical calculations and which have been benchmarked by experiment. The suppression factor is based-upon earlier detailed collision-radiative calculations which were made for a wide range of ions at various densities and temperatures, but used a simplified treatment of DR. A general suppression formula is then developed as a function of isoelectronic sequence, charge, density, and temperature. These density-dependent effective DR rate coefficients are then used in the plasma simulation code Cloudy to compute ionization balance curves for both collisionally ionized and photoionized plasmas at very low ($n_e = 1 \text{ cm}^{-3}$) and finite ($n_e = 10^{10} \text{ cm}^{-3}$) densities. We find that the denser case is significantly more ionized due to suppression of DR, warranting further studies of density effects on DR by detailed collisional-radiative calculations which utilize state-of-the-art partial DR rate coefficients. This is expected to impact the predictions of the ionization balance in denser cosmic gases such as those found in nova and supernova shells, accretion disks, and the broad emission line regions in active galactic nuclei.

Subject headings: suppression

1. Introduction

Astronomical emission or absorption sources have an enormous range of densities. Two examples include the intergalactic medium, with $n_e \sim 10^{-4} \text{ cm}^{-3}$, and the broad emission-line regions of Active Galactic Nuclei, with $n_e \sim 10^{10} \text{ cm}^{-3}$. The gas producing the spectrum is not in thermodynamic equilibrium (Osterbrock & Ferland 2006), so microphysical processes determine the physical conditions.

The two common cases encountered for ionization are photoionization and collisional (e.g., electron-impact) ionization. In both cases, ions are recombined by dielectronic and radiative recombination, with dielectronic recombination (DR) usually the dominant process for elements heavier than helium. Databases give ionization and recombination rates that are the sum of several contributing processes. Examples include Voronov (1997) for electron impact ionization, Verner & Yakovlev (1995) for photoionization, and the DR project (Badnell et al. 2003) for dielectronic recombination and Badnell (2006a) for radiative recombination; it is these latter data ¹ which will be of primary interest to us in the present study.

The collisional ionization and recombination rate coefficients used in astrophysics are frequently assumed to depend on temperature but to have no density dependence. The rigorous treatment of density dependent ionization and recombination rate coefficients is via collisional-radiative modeling. This was introduced by Bates et al. (1962) for radiative recombination only and extended to treat the much more complex case of dielectronic recombination by Burgess & Summers (1969). Summers applied their techniques to determine density dependent ionization and recombination rate coefficients, and the consequential ionization balance for collisional plasmas, for H-like thru Ar-like ions.

¹<http://amdpp.phys.strath.ac.uk/tamoc/DATA/>

Graphical results were presented for the elements C, O and Ne (Summers 1972) and then N, Mg and Si (Summers 1974). Reduced temperatures and densities were used so as to enable easy interpolation for other elements. Tables of such recombination rate coefficients were made available only via a Laboratory Report — Summers (1974 & 1979) — due to their voluminous nature at that point in history. The ‘difficulty’ in utilizing this pioneering data led to some modelers attempting to develop simplified approaches. For example, Jordan (1969) used an approach which was based on truncating the zero-density DR sum over Rydberg states using a simple density dependent cut-off which itself was based on early collisional-radiative calculations by Burgess & Summers (1969); a suppression factor was formed from its ratio to the zero-density value and then used more generally. Also, Davidson (1975) simplified the collisional-radiative approach of Burgess & Summers (1969) and, using hydrogenic atomic data, determined suppression factors for Li-like C IV and O VI. New calculations for C IV were made by Badnell et al. (1993) utilizing more advanced (generalized) collisional-radiative modeling (Summers & Hooper 1983) and much improved atomic data at collisional plasma temperatures (see the references in Badnell et al. (1993)).

All of the above works were for electron collisional plasmas and used rather basic DR data (excluding Badnell et al. (1993)) as epitomized in the Burgess (1965) General Formula, viz. a common dipole transition for dielectronic capture, autoionization, and radiative stabilization. The purpose of the present paper is to explore density suppression of DR in photoionized plasmas, and within collisional plasmas, using state-of-the art DR data which takes account of a myriad of pathways not feasible in the early works above, but which has been shown to be necessary by comparison with experiment. We wish to gain a broad overview utilizing the large test-suite maintained by the plasma simulation code Cloudy. We utilize an approach to DR suppression which is motivated initially by the detailed collisional-radiative results given in Badnell et al. (1993) for C IV at $T = 10^5$ K, along with known scalings to all temperatures, charges, and densities. Using these results as

a guideline, a more general suppression formula is then determined by fitting to suppression results from extensive detailed collisional-radiative calculations (Summers 1974 & 1979) for a wide range of ions at several densities and (high) temperatures. Additional modifications are then introduced to account for low temperature DR.

The outline of the rest of the paper is as follows: in the next section we describe the DR suppression model we use; we then apply this suppression to the zero-density DR data, and use the resultant density-dependent DR data in Cloudy to determine the ionization distribution produced under photoionized and collisional ionization equilibrium at low and moderate densities.

2. Generalized Density Suppression Model

We use the following approach, detailed more fully in the subsections below. First, the high-temperature collisional-radiative modeling results of Badnell et al. (1993) for DR suppression in C IV are parameterized by a pseudo-Voigt profile to study the qualitative behavior of suppression as a function of density and temperature. Next, this formulation is then used as a guideline for developing a more comprehensive suppression formula which is obtained by fitting to collisional radiative data for various isoelectronic sequences, ionic charges, densities, and temperatures (Summers 1974 & 1979). Lastly, the suppression formulation is extended to low-temperatures according to the nature of the sequence-specific DR.

2.1. High-Temperature Suppression for Li-like C IV

We begin by considering DR of Li-like C IV, for which the density dependent total DR rate coefficient, and therefore the suppression factor, has been computed rigorously within

a collisional-radiative modeling approach (Badnell et al. 1993).

In the electron collisional ionization case, because of the consequential high temperature of peak abundance, dielectronic recombination occurs mainly through energetically high-lying autoionizing states (via dipole core-excitations) for which radiative stabilization is by the core electron into final states just below the ionization limit:

$$e^- + 1s^2 2s \rightarrow 1s^2 2pnl \rightarrow 1s^2 2snl + h\nu . \quad (1)$$

In the zero-density limit, the intermediate $1s^2 2snl$ states can only decay further via radiative cascading until the $1s^2 2s^2$ final recombined ground state is reached, thereby completing the DR process:

$$1s^2 2snl \longrightarrow 1s^2 2sn'l' + h\nu_1 \rightarrow \dots \rightarrow 1s^2 2s^2 + h\nu_1 + h\nu_2 + \dots \quad (2)$$

For finite electron densities n_e , on the other hand, there is also the possibility for reionization via electron impact, either directly or stepwise,

$$e^- + 1s^2 2snl \longrightarrow 1s^2 2sn'l' + e^- \rightarrow \dots \rightarrow 1s^2 2s + e^- + e^- , \quad (3)$$

and the probability of the latter pathway is proportional to the electron density n_e . Because of this alternative reionization pathway at finite densities, the *effective* DR rate coefficient $\alpha_{\text{DR}}^{\text{eff}}(n_e, T)$ is thus *suppressed* from the zero-density value $\alpha_{\text{DR}}(T)$ by a density-dependent suppression factor $S(n_e, T)$:

$$\alpha_{\text{DR}}^{\text{eff}}(n_e, T) \equiv S(n_e, T) \alpha_{\text{DR}}(T) . \quad (4)$$

From the earlier detailed studies of Davidson (1975) and Badnell et al. (1993), the suppression factor is found to remain unity, corresponding to zero suppression, at lower densities until a certain *activation* density $n_{e,a}$ is reached, beyond which this factor decreases exponentially from unity with increasing density. We have found that this suppression

factor, as a function of the dimensionless log density parameter $x = \log_{10} n_e$, can be modeled quite effectively by a pseudo-Voigt profile (Wertheim et al. 1974) — a weighted mixture μ of Lorentzian and Gaussian profiles of widths w for densities above the activation density $x_a = \log_{10} n_{e,a}$:

$$S(x; x_a) = \begin{cases} 1 & x \leq x_a \\ \mu \left[\frac{1}{1 + (\frac{x - x_a}{w})^2} \right] + (1 - \mu) \left[e^{-\left(\frac{x - x_a}{w/\sqrt{\ln 2}}\right)^2} \right] & x \geq x_a \end{cases}. \quad (5)$$

Fitting this expression to the suppression factor of Badnell et al. (1993) for C IV (which was computed at $T = 10^5$ K) yielded the values $\mu = 0.372$, $w = 4.969$, and $x_a = 0.608$, and this parameterization formula is found to be accurate to within 5% for all densities considered (see Fig. 1).

2.2. Generalized High-Temperature Suppression Formula

Given the suppression formula for Li-like C IV, corresponding to ionic charge $q_0 = 3$ and temperature $T_0 = 10^5$ K, we wish to generalize this expression to other Li-like ions of charge q and (high) T according to the following qualitative guidelines. It is well known that density effects scale as q^7 — see Bates et al. (1962) and Burgess & Summers (1969). The activation density is attained when the reionization rate in Eq. 3, which depends linearly on the density, becomes comparable to the radiative stabilization rate in Eq. 2. The radiative rate is independent of density and temperature, but scales with charge as $A_r \sim q^4$, whereas the electron-impact ionization rate depends on all three, viz. $n_e \alpha_{eII} \sim n_e q^{-3} T^{-1/2}$. An initial suggestion is that the activation density is attained when these two are approximately equal, i.e.,

$$n_{e,a} q^{-3} T^{-1/2} \sim q^4, \quad (6)$$

indicating that the activation density should scale as $n_{e,a} \sim q^7 T^{1/2}$, if the above qualitative discussion holds. The log activation density for all q and T might therefore be expected to

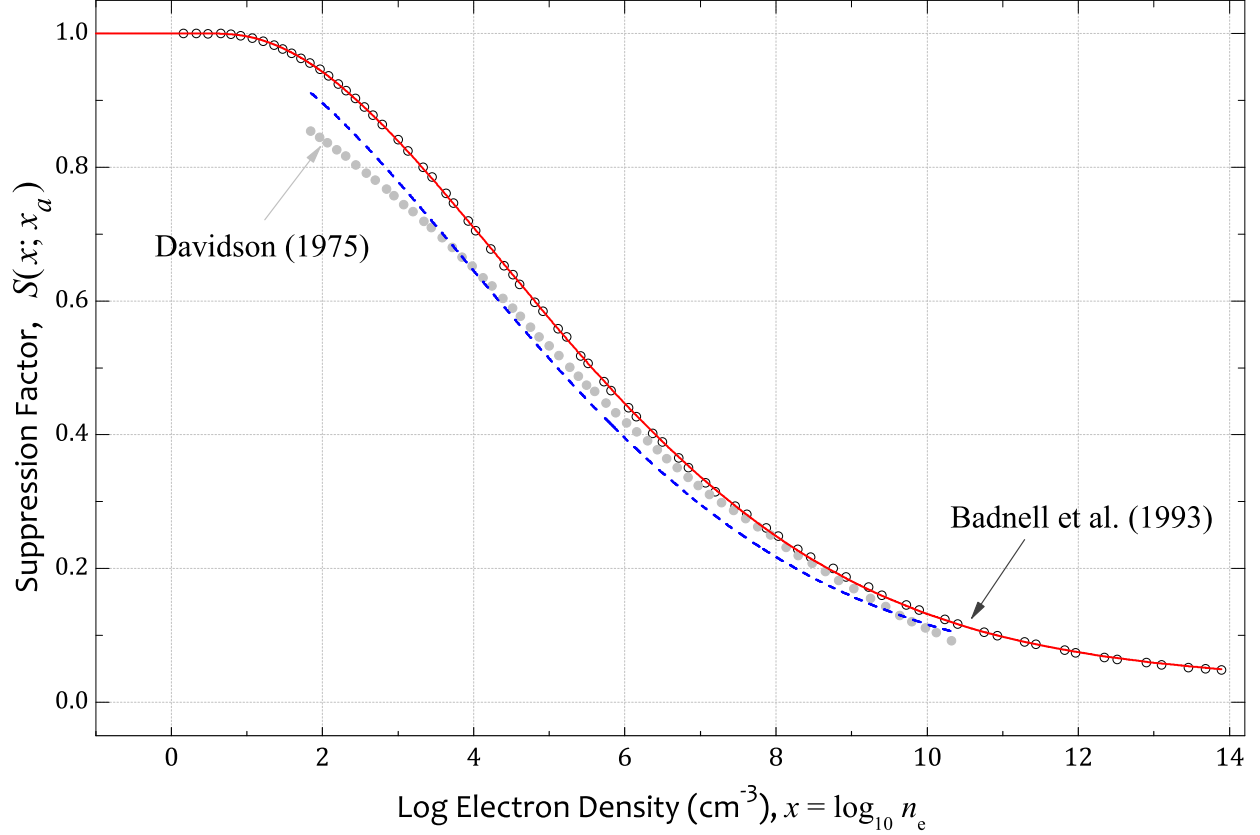


Fig. 1.— Pseudo-Voigt fit of the suppression factor for C IV, as given in Eq. 5 with a scaled activation density as given by Eq. 7, shown for two different temperatures. The red solid curve shows that the parameterization for $T = 1 \times 10^5$ K, corresponding to an activation density of $x_a = 0.608$ (with $\mu = 0.372$ and $w = 4.969$), is in close agreement with the actual data of Badnell et al. (1993) (open circles). The blue dashed curve is the parameterization for $T = 1.5 \times 10^4$ K, using instead an activation density of $x_a = 0.196$ (and the same μ and w), and giving satisfactory agreement with the data of Davidson (1975) (solid circles).

obey the scaling relationship

$$x_a(q, T) = x_a(q_0, T_0) + \log_{10} \left[\left(\frac{q}{q_0} \right)^7 \left(\frac{T}{T_0} \right)^{1/2} \right], \quad (7)$$

where $x_a(q_0, T_0) = 0.608$, $q_0 = 3$, and $T_0 = 10^5$ K are the (log) activation density, the charge, and the temperature for the C IV case treated by Badnell et al. (1993). We note that this expression, when applied to Li-like O VI, gives an increase in the activation density by a factor of $(5/3)^7 = 35.7$, in agreement with the approximate factor of 40 found by Davidson (1975). Furthermore, when scaled in temperature, the formula gives fairly good agreement with the suppression results of Davidson (1975) for C IV at $T = 1.5 \times 10^4$ K (see Fig. 1).

2.2.1. Fit to the Collisional Radiative Data

The preceding treatment reasonably extends the C IV suppression factor at 10^5 K to other high temperatures and to other Li-like ions. However, we need suppression factors applicable to all ionization stages of all elements up to at least Zn for a general implementation within Cloudy. Unfortunately, detailed collisional-radiative modeling data with state-of-the-art DR data is still rather limited. However, extensive tables of effective recombination rate coefficients have been computed by Summers (1974 & 1979) for a wide variety of isoelectronic sequences, charge-states, temperatures, and densities. The treatment of DR there is somewhat simplified, but we only require the *ratio* of finite- to zero-density rate coefficients to determine the suppression factor. We then combine this ratio with our state-of-the-art zero density DR rate coefficients again for use within Cloudy. This ratio is much less sensitive to the specific treatment of DR.

The rather simplistic scaling formula in Eq. 7 was found to be inadequate when applied to the extensive tabulation of suppression factors found in Summers (1974 & 1979). Instead, in order to fit the data accurately, a more generalized formula was arrived at,

146 where a pseudo-Gaussian, corresponding to $\mu = 0$ in Eq. 5, was more appropriate,

$$S^N(x; q, T) = \begin{cases} 1 & x \leq x_a(q, T, N) \\ e^{-\left(\frac{x - x_a(q, T, N)}{w/\sqrt{\ln 2}}\right)^2} & x \geq x_a(q, T, N) \end{cases}. \quad (8)$$

147 Furthermore, the activation density was found to be best represented by the function

$$x_a(q, T, N) = x_a^0 + \log_{10} \left[\left(\frac{q}{q_0(q, N)} \right)^7 \left(\frac{T}{T_0(q, N)} \right)^{1/2} \right], \quad (9)$$

148 where the variables $q_0(q, N)$ and $T_0(q, N)$ are taken to be functions of the charge q and
 149 the isoelectronic sequence, labeled by N . A fit of the suppression factors of Summers
 150 (1974 & 1979) for all ions yielded a global (log) activation density $x_a^0 = 10.1821$ and more
 151 complicated expressions for the zero-point temperature T_0 and charge q_0 . These were found
 152 to depend on both the ionic charge q and the isoelectronic sequence N viz.

$$T_0(q, N) = 5 \times 10^4 [q_0(q, N)]^2 \quad (10)$$

153 and

$$q_0(q, N) = (1 - \sqrt{2/3q})A(N)/\sqrt{q}, \quad (11)$$

154 where

$$A(N) = 12 + 10N_1 + \frac{10N_1 - 2N_2}{N_1 - N_2}(N - N_1) \quad (12)$$

155 depends on the isoelectronic sequence in the periodic table according to the specification of
 156 the parameters

$$(N_1, N_2) = \begin{pmatrix} (3, 10) & N \in 2^{nd} \text{ row} & (37, 54) & N \in 5^{th} \text{ row} \\ (11, 18) & N \in 3^{rd} \text{ row} & (55, 86) & N \in 6^{th} \text{ row} \\ (19, 36) & N \in 4^{th} \text{ row} & (87, 118) & N \in 7^{th} \text{ row} \end{pmatrix}. \quad (13)$$

157 However, even this rather complicated parameterization was inadequate for the lower

158 isoelectronic sequences $N \leq 5$, and for these we explicitly list the optimal values for $A(N)$

in Table 1. Furthermore, at electron temperatures and/or ionic charges for which the q -scaled temperature $\theta \equiv T/q^2$ was very low ($\theta \leq 2.5 \times 10^4$ K), a further modification to the coefficients $A(N)$ for $N \leq 5$ is necessary in that the values in Table 1 should be multiplied by a factor of two.

The above final formulation, which consists of the use of Eq. 8, with $\mu = 0$, $w = 5.64548$, and a rather complicated activation density given by Eqs. 9, 10, 11, 12, and 13, with $x_a^0 = 10.1821$, has been found to model the entire database of ions, temperatures, and densities considered in the Summers (1974 & 1979) data fairly well. To illustrate the general level of agreement over a large range of ions and environments, we compare our parameterized model formulation to the actual suppression data from that report (Summers 1974 & 1979) for a few selected cases in Fig. 2. In order to quantify more fully the extent of agreement, we focus on the case of iron ions, for which we study density effects on ionization balance determination in the next section. A comparison is shown in Fig. 3 between our predicted suppression factors and the data from the Summers (1974 & 1979) report. It is seen that our model fits that data to within 21% for all densities, temperatures, and ionic stages reported (Summers 1974 & 1979). More broadly, we have applied a similar $2 - \sigma$ analysis to *all* ions in that report, at all temperatures and densities, and find the same agreement (20-26% confidence level).

Lastly, it is of interest to investigate how our final suppression factor in Eq. 8 compares to our original, motivating, formulation of Eq. 8 for C IV, shown in Fig. 4. There is generally good qualitative agreement. However, it is seen that the original formulation, based on the Badnell et al. (1993) results, shows a somewhat stronger suppression effect up to $x \approx 11$. This is likely due to the more accurate treatment of the partial DR data of Badnell et al. (1993) entering the collisional-radiative modeling, although some difference due to the collisional-radiative modeling itself may also be present. This indicates that even

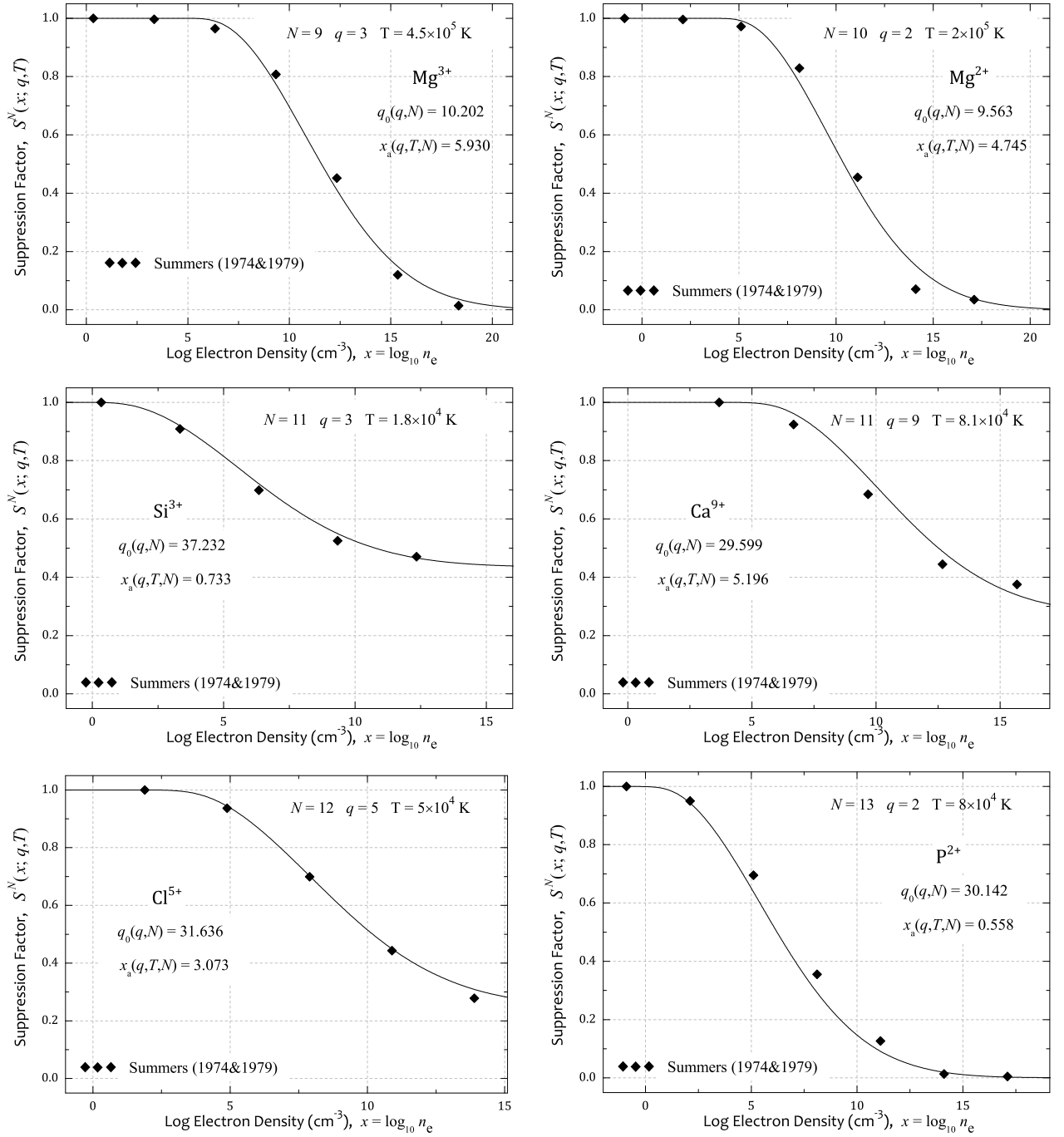


Fig. 2.— A comparison between the present parameterized suppression factor and the collisional radiative results of Summers (1974 & 1979) for a sample of ions and temperatures, as a function of density.

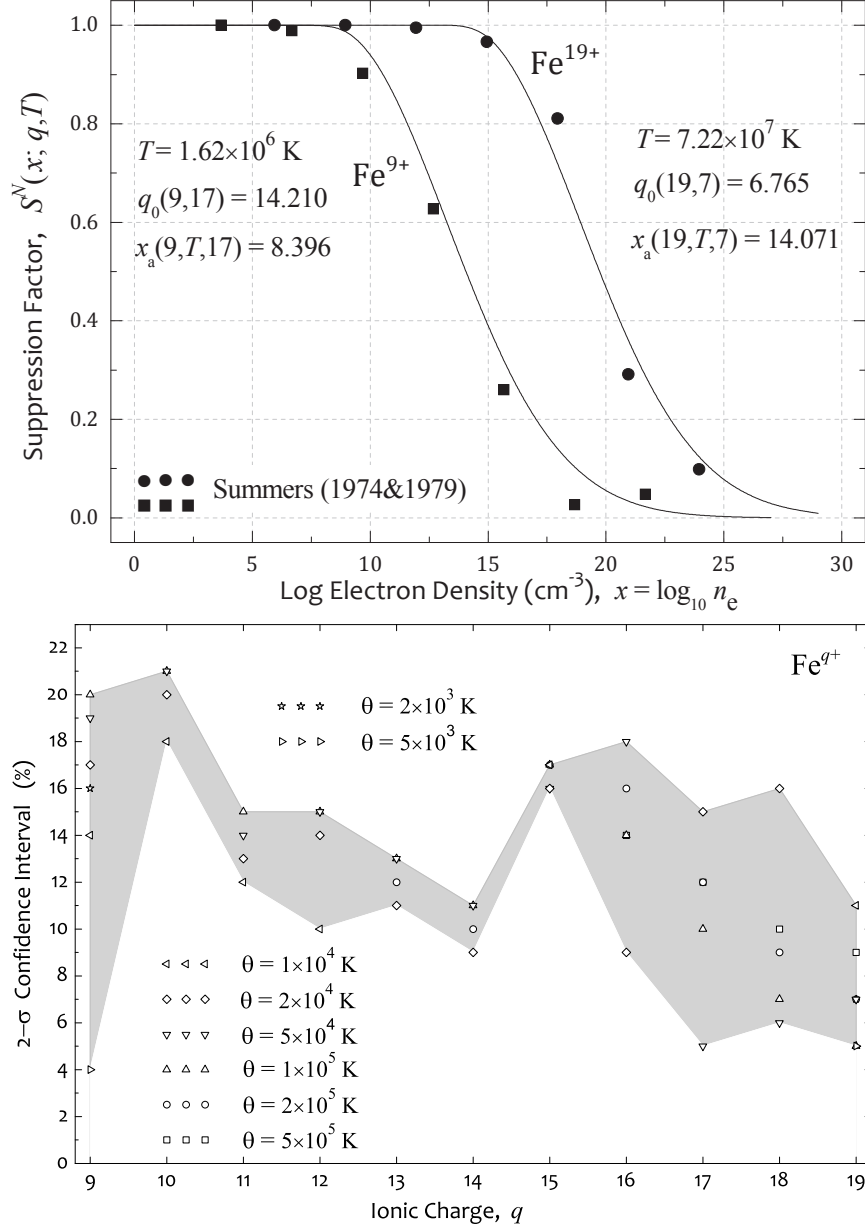


Fig. 3.— Agreement between the suppression curve of Eq. 9 and the Summers (1974 & 1979) data for all iron ions Fe^{q+} , $q = 9 - 19$. The upper panel shows the detailed level of agreement of the two end cases, Fe^{9+} and Fe^{19+} . The lower panel shows the $2 - \sigma$ (95.4%) confidence level as a function of charge state; this means that 95.4% of all density data points in the Summers (1974 & 1979) data, for the given charge and temperature, are within that percentage of the prediction from Eq. 8. The symbols denote different values of the scaled temperature $\theta = T/q^2$.

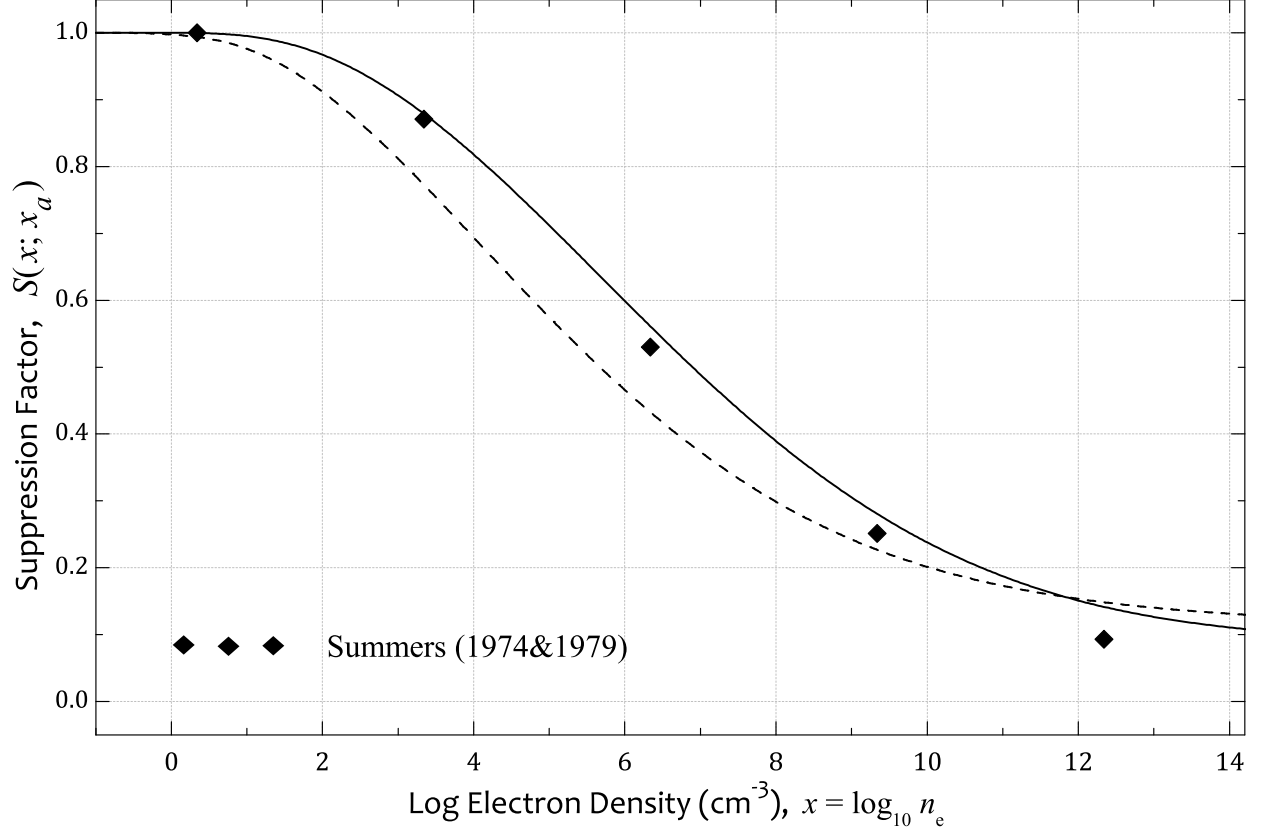


Fig. 4.— A comparison between the final suppression factor of Eq. 8 (solid line), corresponding to a pseudo-Gaussian profile with activation density $x_a = 0.8314$ ($q_0 = 40.284$) and width $w = 5.64548$, the Summers (1974 & 1979) data points (solid diamonds), and the original formulation of Eq. 5 (dashed line), corresponding to a pseudo-Voigt profile with activation density $x_a = 0.608$, width $w = 4.696$, and mixture coefficient $\mu = 0.372$. The temperature $T = 1 \times 10^5$ K is the same as in Fig. 1.

collisional plasmas require collisional-radiative modeling with state-of-the-art DR data. The stronger suppression tails-off at $x \gtrsim 11$ as three-body recombination starts to become relevant and which, at even higher densities (not shown), causes the suppression factor to rise (since it is a ratio of effective recombination rate coefficients, i.e. includes three-body recombination.)

2.3. Suppression Formula at Low Temperatures.

The preceding formulation was based on the suppression factor found by Summers (1974 & 1979) for electron collisionally ionized plasmas, i.e., at higher temperatures, where DR is dominated by high- n resonances attached to a dipole-allowed core excited state. In photoionization equilibrium, however, the temperature at which a given ion forms is substantially smaller than that found in the electron collisional case. Due to the lower kinetic temperatures, DR occurs mainly through energetically low-lying autoionizing states, often via non-dipole core-excitations for which radiative stabilization is by the (outer) Rydberg electron. These states are not, in general, as susceptible to density suppression as their high- n counterparts, and so it may be necessary to modify the preceding suppression formulation.

We first consider sequences with partially-occupied p -subshells in the ground state, which includes the B-like $2p(^2P_{1/2,3/2})$, C-like $2p(^3P_{0,1,2})$, O-like $2p(^3P_{0,1,2})$, F-like $2p(^2P_{3/2,1/2})$, Al-like $3p(^2P_{1/2,3/2})$, Si-like $3p(^3P_{0,1,2})$, S-like $3p(^3P_{0,1,2})$, and Cl-like $3p(^2P_{3/2,1/2})$ systems. For these sequences, there is fine-structure splitting in the ground state and a correspondingly small excitation energy, ϵ_N , giving dielectronic capture into high principal quantum numbers (because of the Rydberg relation $q^2/n^2 \leq \epsilon_N$). Stabilization is via $n \rightarrow n'$ transitions and the recombined final state is built upon an excited parent. Ultimately, it is the strength of collisional coupling of this final state with the continuum

which determines whether recombination or ionization prevails. As the density increases, collisional LTE extends further down the energy spectrum. It is difficult to give a general statement about the position of such final states relative to the ionization limit. So, we assume a worst case scenario, i.e., that such states are subject to suppression, and we use the preceding suppression formula. If density effects are found to be small in photoionized plasmas then this is likely sufficient. If they appear to be significant then a more detailed treatment based on collisional-radiative modeling will be needed. Thus, for these systems, we retain the same suppression formula developed above, that is, $S^N(x, q, T) = S(x, x_a(q, T))$ for $N = \{5, 6, 8, 9, 13, 14, 16, 17\}$, and for all q and T .

For the hydrogenic and the closed-shell He-like and Ne-like cases, on the other hand, the excitations proceed via an increase in core principal quantum number — $1s \rightarrow 2s$ or $\{2s, 2p\} \rightarrow \{3s, 3p, 3d\}$ — giving the dominant dielectronic capture into the low- $n < 10$ resonances. Even following core radiative stabilization, these low-lying states are impervious to collisional reionization for the range of densities $x \leq 10$, and thus we set $S^N(x, q, T) = 1.0$ for $N = \{1, 2, 10\}$. However, at densities $x > 10$, the Summers (1974 & 1979) data for these three isoelectronic sequence show suppression factors that are fit well by the usual Eq. 8, so we do not modify $S^N(x, q, T)$ for these cases.

Lastly, we consider the intermediate isoelectronic sequences for which excitation arises from neither a fine-structure splitting of the ground state nor a change in principal quantum number of the core. These include the Li-like $2s \rightarrow 2p$, Be-like $2s^2 \rightarrow 2s2p$, N-like $2s^22p^3(^4S) \rightarrow 2s2p^4(^4P)$, Na-like $3s \rightarrow 3p$, Mg-like $3s^2 \rightarrow 3s3p$, and P-like $3s^23p^3(^4S) \rightarrow 3s3p^4(^4P)$ cases up through the third row sequences. Any large low-temperature DR contribution arising from near threshold resonances is to low-lying states, for which suppression is negligible, i.e. the high-temperature suppression factor must be switched-off ($S^N \rightarrow 1$) at low- T .

To illustrate the general demarcation between low- T and high- T DR, we first consider DR of C IV, an overview of which is depicted in Fig. 5. The DR cross section, shown in the inset, is dominated by two features. The first is the $n \rightarrow \infty$ accumulation of resonances at the $\epsilon = 8$ eV series limit — those which can be treated in the usual high- T fashion (Burgess 1965; Burgess & Summers 1969) and are therefore susceptible to suppression according to our formulation above. However, there is a second strong contribution from the lowest accessible resonances just above the threshold electron energy, which, according to the Rydberg consideration $3^2/n^2 \approx \epsilon_3 = 0.6$ Ryd, occur here for $n = 4$. More generally, these low-lying states are typical of the low-lying DR spectrum (Nussbaumer & Storey 1984)². The $1s^2 2p 4l$ resonances decay predominantly to the $1s^2 2s 2p$, $1s^2 2p^2$ and $1s^2 2s 4l$ states. These states lie well below the ionization limit and so are not susceptible to further reionization. Since there should be no density suppression then, we seek a modified suppression factor which tends toward unity (i.e., no suppression) at lower temperatures.

In order to make a smooth transition from the high- T suppression factor $S(x; q, T)$ given in Eq. 8, which is appropriate for the high- T peak region $kT \approx kT_{max} = 2\epsilon_N/3$, to the low- T region, where $S^N \rightarrow 1$, we use the modified factor

$$S^N(x; q, T) = 1 - [1 - S(x; q, T)] \exp\left(-\frac{\epsilon_N(q)}{10kT}\right), \quad (14)$$

where $\epsilon_N(q) = 8$ eV for the particular case of C IV ($N = 3$ and $q = 3$). As seen in Fig. 5, the density-dependent effective DR rate coefficient, $\alpha_{DR}^{eff}(n_e, T)$, indeed satisfies the requirement that the high- T peak is suppressed according to the formulation of Badnell et al. (1993) whereas suppression is totally turned off for the lower- T peak.

We have investigated the application of Eq. 14 for all ions that exhibit these same low- T

² We note that the C IV $n = 4$ resonance manifold has been the subject of further near-threshold density-dependent effects (Pindzola et al. 2011).

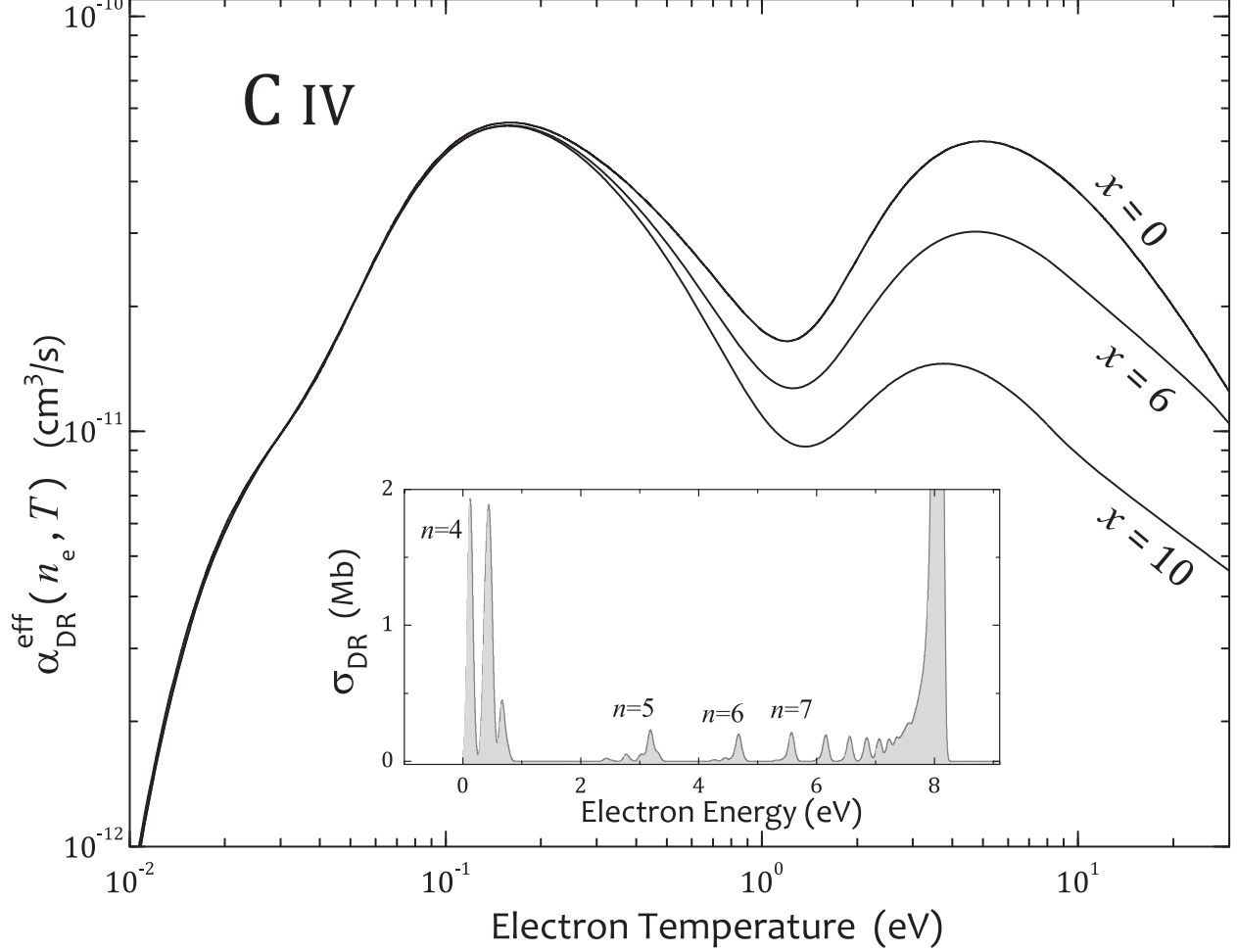


Fig. 5.— DR of C IV. The inset shows the (zero-density) DR cross section convoluted with a 0.1 eV FWHM Gaussian. The spectrum is dominated by two features: the $n = 4$ DR resonance manifold below 1.0 eV and the $n \rightarrow \infty$ Rydberg resonances accumulating at the $2s \rightarrow 2p$ series limit $\epsilon_3(q_0) \approx 8$ eV. The main figure shows the effective DR rate coefficient for several densities. Our modified suppression formulation for $x > 0$, using Eqs. 8 and 14, ensures that the high- T peak, corresponding to the $n \rightarrow \infty$ Rydberg series of resonances, is suppressed but the low- T peak, corresponding to the $n = 4$ resonances, is not suppressed.

resonances features, namely, all isoelectronic sequences $N = \{3, 4, 7, 11, 12, 15\}$, and we have found that the correct transition from suppression at the high- T -peak to no suppression at low- T is indeed satisfied, provided, of course, that the appropriate dipole-allowed excitation energy $\epsilon_N(q)$ is employed. For efficient representation, the excitation energies along each isoelectronic sequence are parameterized by the expression

$$\epsilon_N(q) = \sum_{j=0}^5 p_{N,j} \left(\frac{q}{10} \right)^j . \quad (15)$$

These parameters, which are determined by fitting the above expression to the available NIST excitation energies (Ralchenko et al. 2011), are listed in Table 2.

We note that all isoelectronic sequences and ionization stages are now included in this prescription — our final comprehensive model for treating DR suppression, albeit in a simplified fashion. For those ions with fine-structure splitting in the ground state, we have $\epsilon_N(q) \approx 0$, so that $S^N(x; q, T) = S(x; q, T)$. (We apply this generally also for Ar-like sequences and above ($N \geq 18$), based-on the density of states — see, for example, Badnell (2006b).) For the closed-shell cases, on the other hand, we have $\epsilon_N(q) \rightarrow \infty$. Thus, $S^N(x; q, T) = 1$ for hydrogenic and closed-shell systems, i.e., there is no suppression (for $x \leq 10$). Lastly, for the intermediate cases, the suppression factor is gradually increased toward unity at lower temperatures and begins to admit low- n DR resonances.

3. Results

The suppression factors derived here have been applied to the state-of-the-art total DR rate coefficients taken from the most recent DR database.³ These modified data have been incorporated into version C13 of the plasma simulation code Cloudy, most recently

³<http://amdpp.phys.strath.ac.uk/tamoc/DATA/>

described by Ferland et al. (2013). Cloudy can do simulations of both photoionized and collisionally ionized cases, and we show the effects of collisional suppression on both.

Figure 6 shows the ionization distribution of iron for the collisional ionization case. Figure 7 shows a similar calculation for photoionization equilibrium. Both show two hydrogen densities, 1 cm^{-3} , where collisional suppression of DR should be negligible, and 10^{10} cm^{-3} , where collisional suppression should greatly affect the rates for lower charges and temperatures. The upper panel shows the ionization fractions themselves, for these two densities, while the lower panel shows the ratio of the high to low density abundances.

Cloudy’s assumptions in computing collisional ionization equilibrium, as shown in Figure 6, have been described by Lykins et al. (2012). It is determined by the balance between collisional ionization from the ground state and recombination by radiative, dielectronic, and three body recombination to all levels of the recombined species.

The photoionization case shown in Figure 7 depicts the Active Galactic Nucleus spectral energy distribution (SED), described by Mathews & Ferland (1987), as a function of the ionization parameter

$$U \equiv \frac{\Phi_H}{n_H c}, \quad (16)$$

where Φ_H is the hydrogen-ionizing photon flux, n_H is the density of hydrogen, and c is the speed of light. There is only an indirect relationship between the gas kinetic temperature and the ionization of the gas in this case. Here, the level of ionization is determined by a balance between photoionization by the energetic continuum and the total recombination rate.

The lower panels of Figs. 6 and 7 show that the amount that the ionization increases due to DR suppression can be large — the ratio can easily exceed 1 dex. Clearly, these results demonstrate that density effects on the ionization balance need to be considered

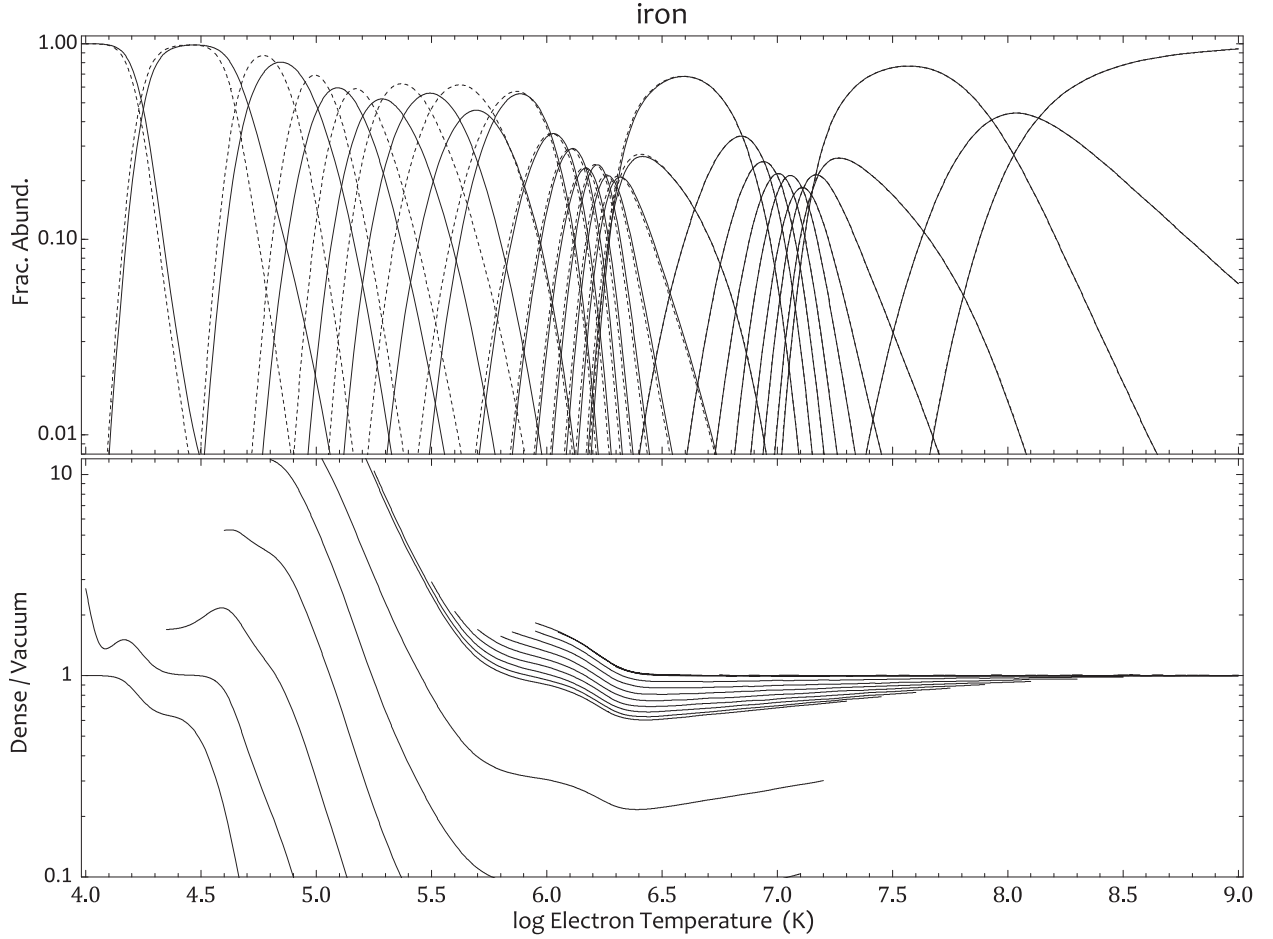


Fig. 6.— Upper panel: collisional ionization fractional abundance vs. electron temperature for all ionization stages of Fe. The solid curves correspond to a density of 1 cm^{-3} and the dashed curves correspond to a density of 10^{10} cm^{-3} . From left to right, the curves range from Fe I to Fe XXVII. Lower panel: ratio of the calculated fractional abundances for the two densities.

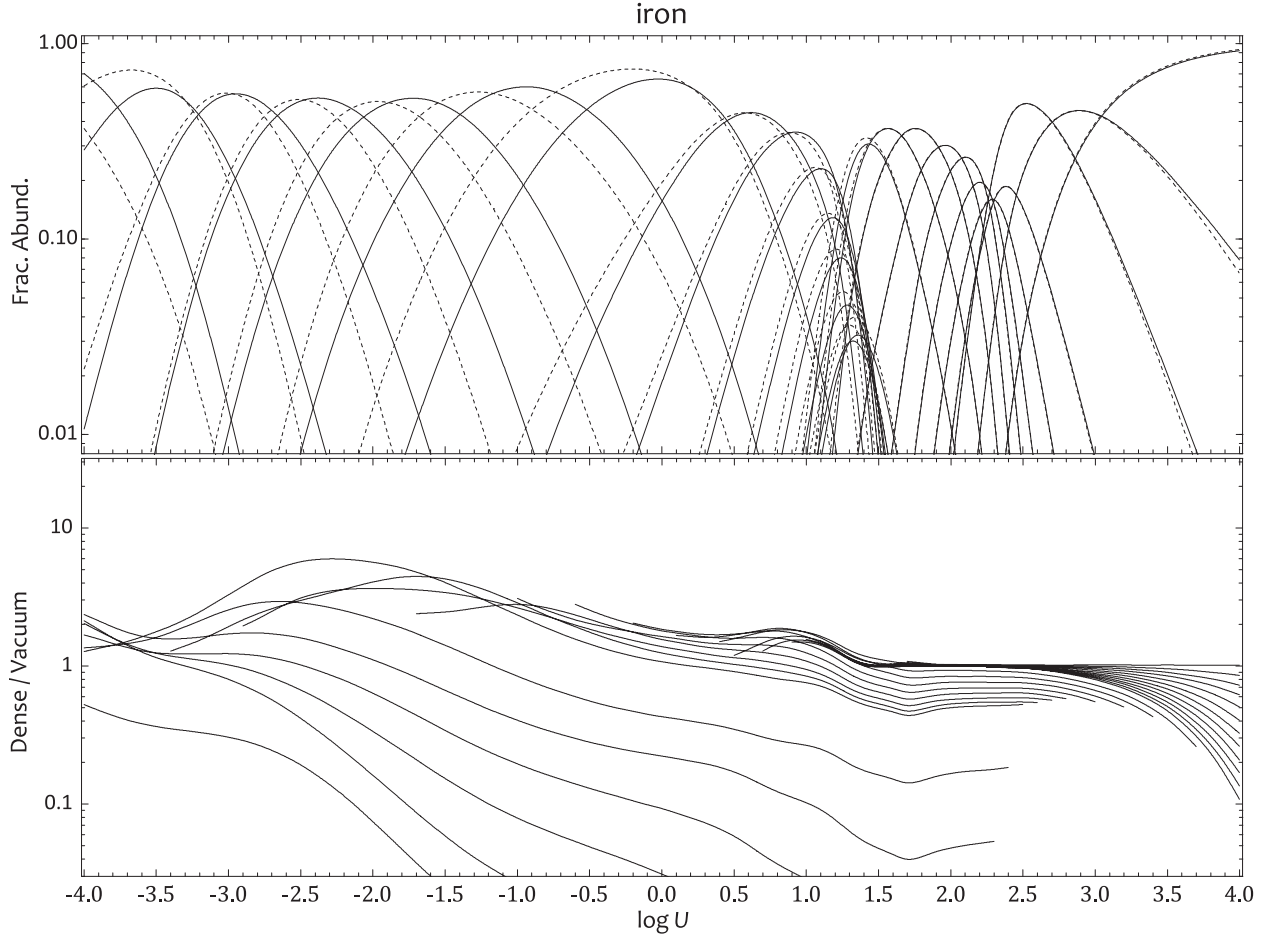


Fig. 7.— Upper panel: photoionization fractional abundance vs. the ionization parameter U for all ionization stages of Fe. The solid curves correspond to a density of 1 cm^{-3} and the dashed curves correspond to a density of 10^{10} cm^{-3} . From left to right, the curves range from Fe I to Fe XXVII. Lower panel: ratio of the calculated fractional abundances for the two densities.

297 more precisely.

298

4. Conclusion

299 We have investigated the effects of finite densities on the effective DR rate coefficients
 300 by developing a suppression factor model, which was motivated by the early work of
 301 Badnell et al. (1993) for C IV and extended to all other ions using physically-motivated
 302 scaling considerations, and more precise fitting of collisional-radiative data (Summers
 303 1974 & 1979). Accurate zero-density DR rate coefficients were then multiplied by this
 304 suppression factor and introduced into Cloudy to study the finite-density effects on
 305 computed ionization balances of both collisionally ionized and photoionized plasmas. It
 306 is found that the difference in ionization balance between the near-zero and finite-density
 307 cases is substantial, and thus there is sufficient justification for further studies of collisional
 308 suppression from generalized collisional-radiative calculations. This is expected to impact
 309 the predictions of the ionization balance in denser cosmic gases such as those found in nova
 310 and supernova shells, accretion disks, and the broad emission line regions in active galactic
 311 nuclei.

312 The present results are intended to be preliminary, and to demonstrate the importance
 313 of density effects on dielectronic recombination in astrophysical plasmas. Given the
 314 approximations adopted, we suggest that their incorporation into models (e.g., via Cloudy)
 315 be used with a little caution. For example, one might run models with and without the
 316 effects of suppression at finite density, especially in modeling higher density plasmas (e.g.,
 317 the broad emission line region in quasars). Nevertheless, it is nearly half a century since
 318 Burgess & Summers (1969) demonstrated significant density effects on DR, and it is time
 319 that some representation exists within astrophysical modeling codes to assess its impact on
 320 the much more rigorous demands made by modern day modeling, especially given its routine

incorporation by magnetic fusion plasma modeling codes. In the longer term, we intend to present results based on detailed collisional-radiative calculations using state-of-the-art state-specific DR rate coefficients.

5. Acknowledgments

DN, TWG, and KTK acknowledge support by NASA (NNX11AF32G). GJF acknowledges support by NSF (1108928; and 1109061), NASA (10-ATP10-0053, 10-ADAP10-0073, and NNX12AH73G), and STScI (HST-AR-12125.01, GO-12560, and HST-GO-12309). UK undergraduates Mitchell Martin and Terry Yun assisted in coding the DR routines used here. NRB acknowledges support by STFC (ST/J000892/1).

REFERENCES

330

331 Badnell, N. R. 2006a, *ApJS*, 167, 334

332 Badnell, N. R. 2006b, *ApJ*, 651, L73

333 Badnell, N. R., O’Mullane, M. G., Summers, H. P., et al. 2003, *A&A*, 406, 1151

334 Badnell, N. R., Pindzola, M. S., Dickson, W. J., et al. 1993, *ApJ*, 407, L91

335 Bates, D. R., Kingston, A. E., & McWhirter, R. W. P. 1962, *Proc. R. Soc. Lond. A*, 267,

336 297

337 Burgess, A. 1965, *ApJ*, 141, 1588

338 Burgess, A. & Summers, H. P. 1969, *ApJ*, 157, 1007

339 Davidson, K. 1975, *ApJ*, 195, 285

340 Ferland, G. J., Porter, R. L., van Hoof, P. A. M., et al. 2013, ArXiv e-prints

341 Jordan, C. 1969, *MNRAS*, 142, 501

342 Lykins, M., Ferland, G. J., Porter, R. L., et al. 2012, *MNRAS*, submitted

343 Mathews, W. G. & Ferland, G. J. 1987, *ApJ*, 323, 456

344 Nussbaumer, H. & Storey, P. J. 1984, *A&AS*, 56, 293

345 Osterbrock, D. E. & Ferland, G. J. 2006, *Astrophysics of Gaseous Nebulae and Active*

346 *Galactic Nuclei*, 2nd edn. (Sausalito, CA: University Science Books)

347 Pindzola, M. S., Loch, S. D., & Robicheaux, F. 2011, *Phys. Rev. A*, 83, 042705

348 Ralchenko, Y., Kramida, A. E., Reader, J., & NIST ASD Team. 2011, National Institute of

349 Standards and Technology, <http://physics.nist.gov/asd>

- 350 Summers, H. P. 1972, MNRAS, 158, 255
- 351 Summers, H. P. 1974, MNRAS, 169, 633
- 352 Summers, H. P. 1974 & 1979, Appleton Laboratory Internal Memorandum IM367 &
353 re-issued with improvements as AL-R-5
- 354 Summers, H. P. & Hooper, M. B. 1983, Plasma Physics, 25, 1311
- 355 Verner, D. A. & Yakovlev, D. G. 1995, A&AS, 109, 125
- 356 Voronov, G. S. 1997, Atomic Data and Nuclear Data Tables, 65, 1
- 357 Wertheim, G. K., Butler, M. A., West, K. W., & Buchanan, D. N. E. 1974, Rev. Sci.
358 Instrum., 45, 1369